

CRISPR-Cas12a targeting of ssDNA plays no detectable role in immunity

Nicole D. Marino^{1,*}, Rafael Pinilla-Redondo^{2,†} and Joseph Bondy-Denomy^{1,3,4,*}

¹Department of Microbiology and Immunology, University of California, San Francisco, San Francisco, CA 94158, USA, ²Section of Microbiology, University of Copenhagen, Universitetsparken 15, 2100 Copenhagen, Denmark, ³Quantitative Biosciences Institute, University of California, San Francisco, San Francisco, CA 94158, USA and ⁴Innovative Genomics Institute, Berkeley, CA 94720, USA

Received November 15, 2021; Revised May 12, 2022; Editorial Decision May 13, 2022; Accepted May 23, 2022

ABSTRACT

CRISPR-Cas12a (Cpf1) is a bacterial RNA-guided nuclease that cuts double-stranded DNA (dsDNA) at sites specified by a CRISPR RNA (crRNA) guide. Additional activities have been ascribed to this enzyme *in vitro*: site-specific (*cis*) single-stranded DNA (ssDNA) cleavage and indiscriminate (*trans*) degradation of ssDNA, RNA, and dsDNA after activation by a complementary target. The ability of Cas12a to cleave nucleic acids indiscriminately has been harnessed for many applications, including diagnostics, but it remains unknown if it contributes to bacterial immunity. Here, we provide evidence that cleavage of ssDNA *in cis* or *in trans* by Cas12a is insufficient to impact immunity. Using LbCas12a expressed in either *Pseudomonas aeruginosa* or *Escherichia coli*, we observed that cleavage of dsDNA targets did not elicit cell death or dormancy, suggesting insignificant levels of collateral damage against host RNA or DNA. Canonical immunity against invasive dsDNA also had no impact on the replicative fitness of co-infecting dsDNA phage, ssDNA phage or plasmid *in trans*. Lastly, crRNAs complementary to invasive ssDNA did not provide protection, suggesting that ssDNA cleavage does not occur *in vivo* or is insignificant. Overall, these results suggest that CRISPR-Cas12a immunity predominantly occurs via canonical targeting of dsDNA, and that the other activities do not significantly impact infection outcomes.

INTRODUCTION

CRISPR-Cas systems are prokaryotic adaptive immune systems that protect bacteria from mobile genetic elements (MGEs), such as phages and plasmids. Six distinct

CRISPR-Cas types (I–VI) have been discovered, all featuring CRISPR-associated (Cas) proteins and a CRISPR array that is established via acquisition of spacers from invasive nucleic acids (1). CRISPR arrays are transcribed and processed into CRISPR RNAs (crRNA) that associate with Cas proteins and direct them to their nucleic acid target (i.e. the protospacer) via complementary base pairing. In addition to sequence-specific targeting of DNA (Type I, II, V) (1) or RNA (Type II, III and VI) (1,2) some CRISPR-Cas systems have been ascribed a ‘collateral damage’ phenotype that leads to the sequence-independent destruction of bystander ssRNA (Type III, VI) (3,4) or DNA (Type III) (5). This indiscriminate cleavage can result in cell death (i.e. abortive infection) or dormancy (6), which prevents viral spread or escape. Bacterial nucleases involved in anti-phage immunity have also been shown to elicit abortive infection by targeting DNA and RNA indiscriminately, including Card1/Can2, Csm6 and NucC (7–10).

Cas12a (Type V-A CRISPR-Cas) is a programmable RNA-guided effector nuclease that creates dsDNA breaks within protospacers next to a protospacer adjacent motif (PAM) (11). Because of its high fidelity, distinct PAM requirements, and relatively short crRNA, Cas12a has been developed as an alternative to Cas9 for gene editing in bacteria, plants, and mammalian cells (12–14). Interestingly, Cas12a also cleaves ssDNA nonspecifically (i.e. *in trans*) upon binding to or cleaving its complementary target (i.e. *in cis*) *in vitro* (15–17). Recognition of the thymine-rich (TTTN) PAM in dsDNA initiates local strand separation and crRNA-target DNA hybridization (i.e. R-loop formation), which triggers conformational activation and exposure of the RuvC catalytic site (18–21). The RuvC domain then cleaves the non-target and target strands in rapid succession (19,20). After cleavage, Cas12a releases the PAM-distal fragment of the target dsDNA but remains bound to the PAM-proximal fragment, which preserves the R-loop and catalytically active state (19,20,22). The exposed RuvC domain is free to cut any ssDNA that fits in its catalytic

*To whom correspondence should be addressed. Email: joseph.bondy-denomy@ucsf.edu

Correspondence may also be addressed to Nicole D. Marino. Tel: +1 415 514 1381; Email: nicole.blackburn-marino@ucsf.edu

†The authors wish it to be known that, in their opinion, the first two authors should be regarded as Joint First Authors.

pocket, regardless of sequence. Notably, this *trans*-state can also be activated *in vitro* by binding complementary ssDNA in a PAM-independent manner (15,16). Other studies have also reported non-specific nicking and degradation of ssRNA and dsDNA *in trans* after Cas12a activation (17,23).

The remarkable ability of Cas12a to degrade ssDNA *in trans* upon activation has led to its rapid development in diagnostics as a DNA endonuclease-targeted CRISPR trans reporter (DETECTR) (15); however, recent work *in vitro* suggests its kinetics were overestimated (24). Nonetheless, the success of these applications and a recent explosion in the functional and evolutionary diversity of the Cas12 (Type V) superfamily have led to a flurry of new detection tools with similar capabilities (25–30). Although the collateral damage observed *in vitro* for these nucleases is well-suited for diagnostics, it raises some concerns about their use in gene therapy (31).

Cas12a *cis*- and *trans*-cleavage *in vitro* has been carefully elucidated using structural and biochemical studies (19–21,32); however no significance of this activity has been described during cellular immunity in bacteria. Bacteria encounter ssDNA in many forms, including bacterial or MGE replication forks and transcription bubbles, ssDNA phages, and dsDNA conjugative elements that transfer through a ssDNA intermediate. Indiscriminate ssDNA cleavage could therefore yield many outcomes: (i) destruction of ssDNA phage or conjugative elements, (ii) targeting of dsDNA phage and plasmid during replication or transcription or (iii) self-targeting during bacterial replication or transcription, possibly resulting in DNA damage response, cell dormancy or death. Indiscriminate cleavage of host RNA or dsDNA upon activation could likewise confer immunity through abortive infection. Here, we provide evidence that Cas12a does not exhibit indiscriminate cleavage activities that impact bacterial immunity. To address these questions, we programmed LbCas12a to target dsDNA phage, ssDNA phage, or conjugated plasmids in *Escherichia coli* or *Pseudomonas aeruginosa*. Although we observed strong canonical immunity against dsDNA phage and plasmid, this did not elicit abortive infection or impact the replicative fitness of co-infecting phage or conjugating plasmid *in trans*. crRNAs complementary to invasive ssDNA also did not provide direct protection. Altogether, these results suggest that cleavage of ssDNA, ssRNA, and host dsDNA does not detectably contribute to immunity in the cell.

MATERIALS AND METHODS

Bacterial strains, plasmids, phages and media

The bacterial strains, plasmids, phages and targets used in this study are described in Supplemental Tables S1 and S2. Bacterial strains were cultured on lysogeny broth (LB) agar or liquid media at 37°C or 30°C as indicated. For *P. aeruginosa* PAO1 strain, extrachromosomal plasmids were maintained using antibiotics at the indicated concentrations: pHERD30T and derivatives, 50 µg/ml gentamicin; pKJK5 (pTrans), 60 µg/ml trimethoprim. For *E. coli* strains, extrachromosomal plasmids were maintained as follows: pHERD20T, 100 µg/ml carbenicillin (strain BW25113); pHERD30T and derivatives, 15 µg/ml gentamicin, pKJK5 (pTrans), 50 µg/ml kanamycin (strains S17-

1 and CSH26). The following strains were grown in media supplemented with antibiotics: *E. coli* S17-1: 30 µg/ml streptomycin; *E. coli* CSH26: 100 µg/ml rifampicin, 100 µg/ml nalidixic acid; PAO1 tn7::LbCas12a attB::crRNA24, 50 µg/ml tetracycline. Inducers were added to the media at the following concentrations: 1 mM IPTG and 0.3% arabinose unless otherwise indicated. M13 phage was purchased from ATCC. λ_{vir} was a gift from Ry Young, and Pf4 phage was a gift from Paul Bollyky.

Construction of plasmids and strains

To generate the PAO1 tn7::LbCas12a strain (Supplementary Figure S1), LbCas12a was first amplified from pMBP-LbCas12a (Addgene #113431) and cloned into pUC18-mini-Tn7T-lac. pUC18-Tn7T-LbCas12a was co-electroporated with pTNS3 plasmid into the *P. aeruginosa* PAO1 strain according to previously published protocols (33,34). The resulting transformants were plated on LB agar supplemented with 30 µg/ml gentamicin to select for integration of the pUC18-Tn7T-LbCas12a vector into the bacterial chromosome. Colonies were screened for integration at the attTn7 site and cured of the gentamicin-resistance cassette using Flp-mediated marker excision, as previously described (33). Clones sensitive to gentamicin were then passed serially in LB to cure them of pFLP2 and render them sensitive to carbenicillin.

crRNAs complementary to DMS3 and JBD30 phages or RFP control were cloned into the HindIII and NcoI sites of pHERD30T. For experiments in which plasmid-borne crRNAs were used, the resulting plasmids were introduced into PAO1 tn7::LbCas12a directly via electroporation and selection on LB supplemented with 50 µg/ml gentamicin. To integrate crRNAs into the chromosome, the region encompassing the *araC* gene, pBAD promoter, and crRNA was amplified from pHERD30T-crRNA vectors and cloned into the mini-CTX2 vector. The resulting plasmids were electroporated into the PAO1 tn7::LbCas12a strain, and integration into the chromosome was selected for using 15 µg/ml tetracycline according to established protocols (35).

To generate the *E. coli* BW25113 F' strain, BW25113 was first mated with TOP10F *E. coli* and plated on M9 minimal media supplemented with 10 µg/ml tetracycline to select for retention of F' in BW25113 and death of the TOP10F leu-autotroph. LbCas12a was amplified from pMBP-LbCas12a and cloned into pTN7C185. The resulting pTN7-LbCas12a vector and pTNS3 were introduced into BW25113 F' via tri-parental mating, and integration of pTN7-LbCas12a into the BW25113 F' chromosome was selected by plating cells on LB supplemented with 10 µg/ml gentamicin (Supplementary Figure S1). Colonies were screened for vector integration into the Tn7 site. crRNAs complementary to λ_{vir} or M13 were cloned into the NcoI and HindIII sites of pHERD20T and introduced into BW25113 F' via chemical transformation.

Liquid culture phage infections

Overnight cultures of *P. aeruginosa* were diluted 1:100 in LB supplemented with 10 mM MgSO₄, 1 mM IPTG, 0.3% arabinose and 50 µg/ml gentamicin. 90 µl of diluted bacte-

ria were then infected with 10 μ l DMS3 phage diluted ten-fold in SM phage buffer in a 96-well Costar plate. These infections proceeded for 24 hours in a Synergy H1 microplate reader with continuous, double orbital shaking at 37°C. PAO1 tn7::LbCas12a pHERD30T-crRNA-RFP was used as the non-targeting control and PAO1 tn7::LbCas12a pHERD30T-crRNA-DMS3 was used for targeting. Dilutions of bacteria and phage were plated to determine the number of colony forming units (CFUs) and plaque forming units (PFUs), respectively. The multiplicity of infection was determined by dividing the number of PFUs by CFUs.

Generation of phage escapers

High titer preparations of JBD30 phage (which encodes the same protospacer present in DMS3) were mixed with overnight cultures of PAO1 tn7::LbCas12a attB::crRNA-DMS3 in top agar and plated on LB supplemented with 1 mM IPTG and 0.3% arabinose. Cultures were grown overnight at 30°C, and resulting plaques were isolated with a sterile pipette tip and resuspended in SM phage buffer with chloroform. The resulting phages were plaqued twice on targeting media and tested for plaque formation on targeting and non-targeting strains. The protospacer regions of *bona fide* phage escapers and wildtype phage were Sanger sequenced and aligned using EMBOSS Needle.

Phage plaque assays

Bacterial lawns were generated by adding 150 μ l bacteria from an overnight culture to 4 ml of 0.7% top agar and spreading the mixture on LB agar supplemented with 10 mM MgSO₄ (*P. aeruginosa*) or 10 mM MgSO₄ and 5 mM CaCl₂ (*E. coli*). Phages were diluted in SM phage buffer (JBD30 and DMS3) or LB supplemented with 10 mM MgSO₄ and 5 mM CaCl₂ (λ_{vir} and M13). 3 μ l of phage was spotted onto bacterial lawns and grown at 30°C or 37°C overnight, respectively. The identity and protospacer sequences of phage stocks were confirmed by PCR and Sanger sequencing.

Rifampicin resistance assay

Overnight cultures of PAO1 tn7::LbCas12a pHERD30T-crRNA-DMS3 were diluted 1:100 in inducing media [LB supplemented with 10 mM MgSO₄, 1 mM IPTG, 0.3% arabinose and 50 μ g/ml gentamicin]. 1 ml cultures were immediately infected with ten-fold serial dilutions of DMS3 phage or buffer as a control. At 16 hours post-infection, saturated cultures were plated directly on LB supplemented with 62 μ g/ml rifampicin or diluted and plated on LB (36). Bacterial CFUs and phage PFUs were plated immediately after infection to determine MOI. Saturated cultures were plated in triplicate at the end of each experiment.

Plasmid conjugation assay

Plasmid conjugation assays were carried out as solid surface filter matings. Five different *E. coli* S17-1 plasmid-mobiliser strains (donors) were independently mated with the two recipient strains in triplicate. Wild type PAO1 (wt)

or PAO1 tn7::LbCas12a attB::crRNA-DMS3 was used as the recipient strain. Each donor strain carried unmodified pHERD30T or a derivative encoding the complementary protospacer sequence on the leading strand (LDS) or lagging strand (LGS) with or without a PAM (Supplementary Figure S3). The strains were grown overnight in LB broth supplemented with the appropriate antibiotics and CRISPR-Cas inducers. Donor and recipient cell suspensions (500 μ l) were washed three times, mixed at a 1:1 ratio and spun down. The pellet was then resuspended in 100 μ l LB and transferred onto sterile 0.2 μ m nitrocellulose filters (Avantec) placed over nonselective LB agar plates with inducers. The bacterial mating mixtures were incubated for 3 h at 37°C to allow conjugation. Filters were then washed with 2 ml PBS to recover cells. Serial dilutions were subsequently plated on selective LB-agar plates with appropriate antibiotics (and no inducers) to discriminate between donor, recipient and transconjugant colony forming units (CFUs). The frequency of plasmid transfer was calculated by dividing the number of transconjugant CFUs by the number of donor CFUs.

Plasmid co-conjugation assay

The co-conjugation experiments were performed as solid surface filter matings in triplicate using *E. coli* strains S17-1 and CSH26 as donors and PAO1 tn7::LbCas12a attB::crRNA-DMS3 (targeting) as the recipient. The pTrans plasmid was simultaneously conjugated with pTarget (which encodes a complementary protospacer) or pTarget(-PS) (which lacks a complementary protospacer), into the recipient strains. Donor and recipient strains were grown overnight using the appropriate selection and CRISPR-Cas induction (recipient only). The donor and recipient cell suspensions (500 μ l) were washed 3 times, mixed at a 1:1:1 ratio and spun down. The pellet was then resuspended in 100 μ l LB and transferred onto sterile 0.2 μ m nitrocellulose filters (Avantec) placed over nonselective LB agar plates with inducers and no antibiotic selection. The bacterial mating mixtures were incubated for 3 h at 37°C to allow conjugation. Filters were then washed with 2 ml PBS to recover cells. Serial dilutions were subsequently plated on selective LB-agar plates with appropriate antibiotics to discriminate between donor, recipient and transconjugant CFUs. The frequency of plasmid transfer was calculated by dividing the number of transconjugant CFUs by the number of donor CFUs.

In vitro transcription

crRNAs were synthesized for *in vitro* cleavage experiments using the HiScribe T7 Quick High Yield RNA Synthesis Kit (New England Biolabs; NEB). Templates for *in vitro* transcription were generated by hybridizing a ssDNA oligo with the T7 promoter to another oligo with the complementary T7 promoter sequence fused to the LbCas12a repeat and spacer in annealing buffer. Approximately 1 μ g template was added to the HiScribe reaction and incubated at 37°C for 16–18 h. Reactions were purified using the Qiagen miRNeasy kit and resulting concentrations were measured using Qubit RNA Broad Range Assay Kit (Thermo Fisher)

and the Qubit Fluorometer (Invitrogen). Purified RNA was loaded onto TBE–urea gels (BioRad) and resolved by electrophoresis in TBE buffer with low range ssRNA ladder (NEB). Gels were post-stained with SYBR gold for 1 h at room temperature and imaged using BioRad Gel Doc EZ Imager.

Phage propagation and purification

LB broth (3 ml) was inoculated with a colony of PAO1 and grown for 4 h, 37°C at 200 revolutions per minute (rpm). High-titer Pf4 phage stock was used to infect each culture (except for one uninfected control). Infected cultures were grown for an additional 1–2 h and transferred to a flask with 75 ml LB broth for 24–48 h, 37°C at 250 rpm. Cells were harvested by centrifugation at 8000 × g for 10 min, 4°C. The supernatant was collected and treated with 1 µg/ml DNase I for 2 h, 37°C. Cells were centrifuged again at 8000 × g for 10 min, 4°C and filter sterilized with a 0.22 µm filter. The filtrate was supplemented with 5 M NaCl and incubated at 4°C for 4 h. Polyethylene glycol (PEG 8000) was added at a final concentration of 4% (w/v), and the sample was left gently rotating at 4°C overnight. To pellet phage, the samples were centrifuged at 13 000 × g for 20 min at 4°C. Pellets were resuspended in 30 ml 10mM Tris 1 mM EDTA, pH 8.0 (TE) buffer and centrifuged again at 15 000 × g at 4°C. The supernatant was collected and supplemented with a quarter-volume of 20% PEG 8000 and 2.5 M NaCl and left overnight at 4°C. Phage was harvested by centrifuging at 15 000 × g, 4°C, 20 min. The resulting pellets were resuspended in 2 ml PBS and dialyzed overnight at 4°C in 1 l PBS using SnakeSkin 10 000 MWCO dialysis tubing (Thermo Fisher). Buffer was refreshed and samples were dialyzed again overnight. Virion viability and yield was determined by plaque assay on PAO1.

M13 was propagated by first infecting BW25113 F⁺ in LB and shaking at 200 rpm at 37°C for 4–5 h. Cleared cultures were then passed through a 0.45 µm filter and stored at 4°C.

Genomic DNA extraction

DNA from purified Pf4 virions was extracted by mixing phage preparations 1:1 in lysis solution (0.4% sodium dodecyl sulfate, 400 µg/ml Proteinase K, 200 µg/ml RNase A) and incubating at 37°C for 1 h. Samples were then incubated at 50°C for 30 min, supplemented with 0.2M NaCl, and subjected to a standard phenol-chloroform extraction. PAO1 genomic DNA was extracted from saturated cultures using the Qiagen DNeasy Ultraclean Microbial Kit according to the manufacturer's instructions. M13 ssDNA was extracted by precipitating phage virions with PEG 8000 and resuspending the phage pellet with phenol per established protocol (37). ssDNA was precipitated with ethanol in the presence of 0.3 M sodium acetate, washed with cold 70% ethanol and resuspended in water.

In vitro cleavage experiments

In vitro Cas12a cleavage assays were performed using EnGen Lba Cas12a (NEB #M0653T) and crRNAs that were synthesized commercially (IDT) or with the HiScribe T7

Quick High Yield RNA Synthesis Kit (NEB). dsDNA templates were amplified from plasmids and purified using DNA Clean and Concentrator Kit (Zymo). 30 nM EnGen LbCas12a was pre-incubated with 30 nM crRNA in NEB-uffer 2.1 for 10 min at 25°C. Substrate DNA (i.e. dsDNA template, M13 ssDNA or Pf4 DNA) was added and incubated at 37°C for 2 h. 1 µl Proteinase K (50 mg/ml) was added and the reaction was incubated at room temperature for 10 min. In vitro cleavage experiments using shrimp ds-DNAse (NEB; EN0771), EcoRI-HF (NEB; R3101S), and Exonuclease I (NEB; M0293S) were performed for 2 h at 37°C and heat inactivated at 65°C. Reactions were loaded onto 1% TAE agarose gels and resolved by electrophoresis. Gels were post-stained with SYBR Gold (Invitrogen) for 1 h at room temperature and imaged using BioRad Gel Doc EZ Imager.

RESULTS

Cas12a targeting does not elicit abortive infection or prevent escaper phage emergence

Diverse orthologs of Cas12a have been shown to *cis*- and *trans*-cleave ssDNA *in vitro*, including LbCas12a (*Lachnospiraceae* bacterium ND 2006), AsCas12a (*Acidaminococcus* sp. BV3L6) and FnCas12a (*Francisella novicida*) (15–17). The bacteria in which these orthologs are naturally found are either genetically intractable or lack known plasmids and phages that can be manipulated to assess *cis*- and *trans*-cleavage. Therefore, we engineered the *P. aeruginosa* lab strain PAO1 to express IPTG-inducible LbCas12a from the chromosome and arabinose-inducible crRNAs programmed to target phage (Supplementary Figure S1). *P. aeruginosa* has previously been used as a host for MbCas12a (*Moraxella bovoculi*) to target phage and identify anti-CRISPR proteins (38).

To determine if Cas12a triggers abortive infection upon cleaving its complementary target, we first infected targeting and non-targeting strains of *P. aeruginosa* with phage DMS3 at varying multiplicities of infection (MOI) and assessed bacterial growth over time (Figure 1A). Cleavage of this protospacer elicits non-specific ssDNA *trans*-cleavage *in vitro* (Figure 1B) and may trigger abortive infection in cells by *trans*-cleaving host nucleic acids. If so, infecting cells with a high MOI (in which most cells are infected) would cause population collapse before phage replication is complete. We observed no significant deviation in the growth kinetics across varying MOIs during this experiment (Figure 1A). Notably, Cas12a immunity was incredibly robust, protecting cells across a 10⁷-fold MOI range. Alternatively, indiscriminate cleavage of ssDNA in replication forks or transcription bubbles could cause mutations in the host genome without triggering abortive infection, as observed with Type III CRISPR-Cas (39). To test for this, we measured rates of resistance to rifampicin, which inhibits DNA-dependent RNA polymerase. Mutations in *rpoB* confer resistance to rifampicin, which can therefore be measured to assess rates of mutagenesis. We observed similar rates of spontaneous rifampicin resistance as previous reports (36,40); however, Cas12a targeting did not increase the rate of rifampicin resistance in the surviving population relative to the uninfected control (Supplementary Figure S2).

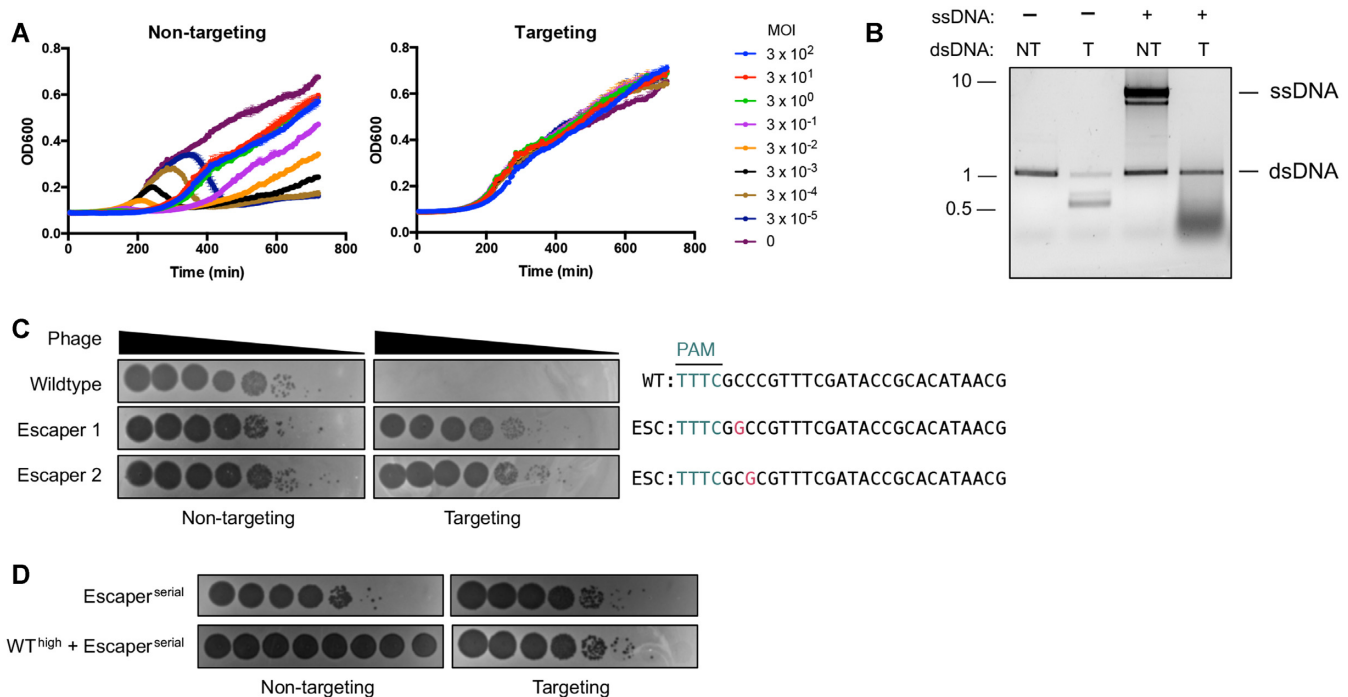


Figure 1. Cas12a targeting does not elicit abortive infection or prevent the rise of phage escapers. (A) Growth curves of *P. aeruginosa* PAO1 tn7::LbCas12a strain expressing targeting or non-targeting crRNAs infected with ϕ DMS3 at multiplicities of infection (MOI) indicated in legend. (B) *In vitro* LbCas12a *cis*- and *trans*-cleavage assay with dsDNA template (plus or minus PAM) and ssDNA. dsDNA template encodes same protospacer encoded in ϕ DMS3 for experiments in (A). (C) Phage plaque assays with ten-fold serial dilutions of wildtype or mutated ϕ JBD30 phage. Bacterial clearance (black) indicates phage replication. Sequences of the targeted phage gene show mutated nucleotides (magenta) in phages able to escape Cas12a targeting. (D) Phage plaque assays in which targeting and non-targeting strains were infected with ten-fold serial dilutions of escaper phage alone or with escaper phage and a high titer of targeted wildtype phage. PAM, protospacer adjacent motif (teal); WT, wildtype phage; ESC, escaper phage. NT, non-target due to lack of PAM; T, target with PAM.

Due to the strength of immunity and the absence of detectable cell dormancy or death, phage escapers emerged from high MOI infections (Figure 1C). These escaper phages had single point mutations in the +2 or +3 position of the seed (PAM-proximal) region of the protospacer, which is consistent with the high sequence fidelity required in this region for successful targeting (11,41). To determine if successful targeting triggers indiscriminate cleavage or nicking of phage nucleic acids, we co-infected cells with wildtype and escaper phage or escaper phage alone (Figure 1D). Infections with high titers of wildtype phage did not detectably impact plaque formation by escaper phages, indicating insignificant levels of collateral damage. Altogether, these data show that active LbCas12a does not induce abortive infection or prevent the emergence of escapers.

Cas12a does not *cis*-cleave invasive ssDNA in cells

We next tested the ability of Cas12a to cleave ssDNA in cells through direct complementary base pairing. We exposed cells to plasmids and ssDNA phages, which enter and exit the bacterium as ssDNA but replicate via a dsDNA intermediate (42). First, we performed conjugation assays using plasmids with the complementary protospacer on the leading or lagging strand. Only the leading strand transfers as ssDNA from the donor to the recipient cell during conjugation; therefore, only plasmids with the complemen-

tary sequence on the leading strand should be susceptible to Cas12a ssDNA cleavage. Because Cas12a requires the PAM for dsDNA unwinding but not conformational activation, we used target constructs with or without the PAM to discriminate between cleavage of dsDNA and ssDNA, respectively (Figure 2A and Supplementary Figure S3). As expected, LbCas12a targeted conjugated plasmid with PAM(+) protospacers regardless of the orientation, which is consistent with cleavage of the dsDNA form (Figure 2A and Supplementary Figure S4). However, we did not detect any targeting of conjugated plasmids with PAM(-) protospacers present on the leading or lagging strand, suggesting the ssDNA strand was not significantly cleaved upon entering the cell.

We then sought to perform ssDNA cleavage experiments in *P. aeruginosa* using the filamentous phage Pf4, which similarly enters and leaves the cell as linear ssDNA and replicates as a dsDNA intermediate (43,44). We infected our model strain with varying titers of Pf4 and again observed targeting only when using crRNAs corresponding to PAM(+) (i.e. dsDNA) protospacers (Supplementary Figure S5), suggesting the absence of *cis* ssDNA targeting. However, we found that DNA purified from Pf4 virions was surprisingly recalcitrant to *trans*-cleavage *in vitro* (Supplementary Figure S5D). We attempted to confirm the single-stranded nature of the phage DNA using a panel of nucleases, with PAO1 genomic DNA included for comparison. Surprisingly, we found that DNA purified from Pf4 was sus-

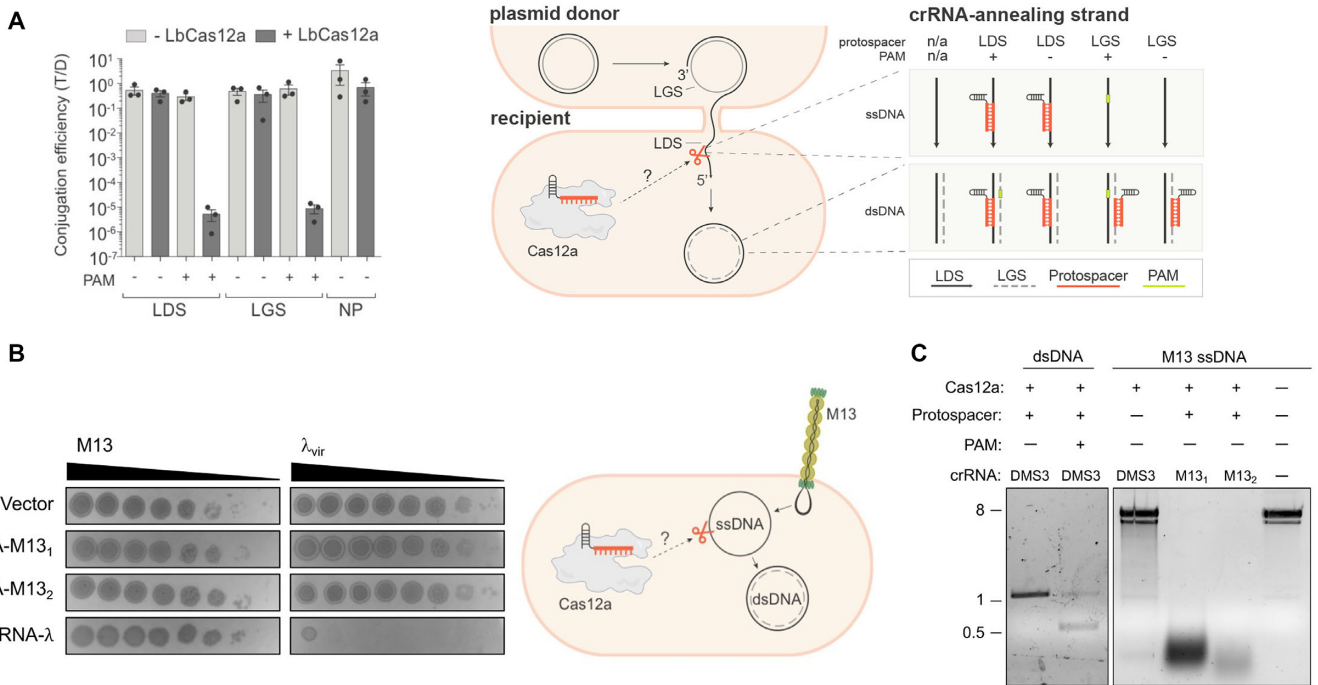


Figure 2. Cas12a does not detectably *cis*-cleave invasive ssDNA in bacteria. (A) Conjugation efficiency for plasmid *cis*-targeting in *P. aeruginosa* PAO1 strain. During conjugation, the donor is nicked and the leading strand (LDS) is transferred as ssDNA to the wildtype (-LbCas12a) or LbCas12a-expressing (+LbCas12a) recipient cell via the mating pilus. LbCas12a was co-expressed with crRNAs complementary to a DMS3 protospacer cloned into the leading (LDS) or lagging (LGS) strand, with (+) or without (-) the correct protospacer adjacent motif (PAM). T/D indicates the ratio of transconjugants to donors. Data are presented as mean \pm SEM ($n = 3$). LDS, complementary protospacer is on leading strand; LGS, complementary protospacer is on lagging strand; NP, no protospacer on plasmid. (B) Plaque assay for phage *cis*-targeting in *E. coli* BW25113 F' strain. Bacterial lawns were infected with dsDNA λ_{vir} or with M13, which enters and leaves the cell as ssDNA but replicates via a dsDNA intermediate. LbCas12a was co-expressed in bacteria with crRNA complementary to M13 positive strand (without PAM) or λ_{vir} (with PAM) during phage infection. Bacterial clearance (black) indicates phage replication. (C) *In vitro* LbCas12a cleavage assay on dsDNA template encoding DMS3 protospacer or M13 ssDNA.

ceptible to dsDNAse but not exonuclease I, which cleaves linear ssDNA nonspecifically (Supplementary Figure S5E and F). Although DNA purified from Pf4 resolved around the expected size (12.4 kb) (45) and was smaller than PAO1 genomic DNA, its susceptibility to EcoRI and dsDNAse suggests that the genome harvested is similar to dsDNA. As a result, we could not definitively conclude the nature of this DNA or the suitability of this phage for assessing ssDNA cleavage.

We therefore established a second bacterial model for LbCas12a in the *E. coli* strain BW25113 F' and used dsDNA phage λ_{vir} and ssDNA phage M13 to assess cleavage activities. M13, like Pf4, is a filamentous phage that enters and exits the bacterium as ssDNA but replicates as dsDNA via rolling-circle replication (46,47). M13 ssDNA is rapidly degraded *in cis* and *in trans* by LbCas12a *in vitro* (15–17) and M13 has been used as a model for Type I-E CRISPR-Cas acquisition and targeting in *E. coli* (48). As with our *P. aeruginosa* model, we engineered *E. coli* to express IPTG-inducible LbCas12a from the chromosome and arabinose-inducible crRNAs (Supplementary Figure S1). When we expressed crRNAs complementary to PAM(+) protospacers in λ_{vir} , we saw a 10⁷-fold reduction in phage titer (Figure 2B). When we expressed crRNAs complementary to PAM(-) protospacers in M13, however, we saw no reduction in plaque formation, even though these same crRNAs enabled cleavage of M13 ssDNA *in vitro* (Figure 2B and

C). These results indicate that LbCas12a readily targets dsDNA, but not ssDNA phage or plasmids in cells, suggesting that the robust degradation of M13 ssDNA observed *in vitro* does not recapitulate during bacterial infection.

Cas12a does not *trans*-cleave invasive ssDNA in cells

Although we could not detect *cis* ssDNA cleavage, we next probed for *trans* ssDNA cleavage that could result after cleavage of a dsDNA target. To this end, we simultaneously conjugated two plasmids—pTarget, which has the correct protospacer and PAM, and pTrans, which has no protospacer—into the same recipient cells and selected for transconjugants using antibiotic selection specific to each plasmid. As a control, we used pTarget(-PS), which is identical to pTarget but lacks the protospacer and PAM. If cleavage of plasmid with the correct target elicits indiscriminate immunity against ssDNA, the number of Cas12a-expressing transconjugants retaining pTrans should be lower during co-conjugation with pTarget than for the pTarget(-PS) control. While conjugation of pTarget was decreased by > 3 orders of magnitude relative to pTarget(-PS), this did not impact pTrans acquisition (Figure 3A, Supplementary Figure S6). We then tested for *trans*-cleavage of ssDNA phage by singly infecting or co-infecting *E. coli* with dsDNA phage λ_{vir} and ssDNA phage M13. When we expressed LbCas12a and λ_{vir} -targeting crRNA

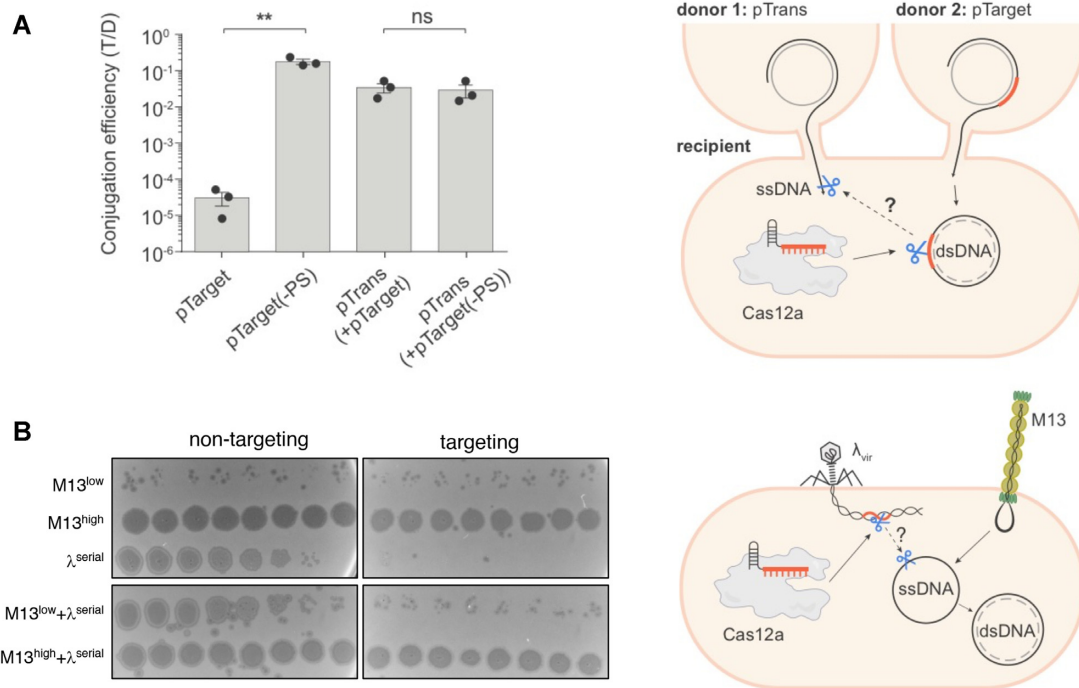


Figure 3. Cas12a does not *trans*-cleave invasive ssDNA in bacteria. (A) Right: Schematic for plasmid co-conjugation and cleavage in *P. aeruginosa* PAO1 strain. Two plasmids were conjugated simultaneously from different donors into the same recipient cell. LbCas12a was co-expressed in the recipient cell with crRNA complementary to pTarget but not pTrans. A parallel co-conjugation mating using pTrans and pTarget(-PS) (identical to pTarget but lacking the protospacer and PAM) was carried out as a control. Conjugation efficiency was assessed using antibiotic selection specific to each plasmid and represented as the transconjugant to donor ratio (T/D). Data are presented as mean \pm SEM ($n = 3$); ** $P = 0.0036$ by unpaired, two-sided Student's t test; ns, not significant ($P > 0.05$) (B) Right: Schematic for phage co-infection in *E. coli*. Bacterial lawns of *E. coli* BW25113 F' strain co-expressing LbCas12a and λ -targeting or non-targeting crRNA were singly infected or co-infected with ssDNA phage M13 and dsDNA phage λ_{vir} . Strains were infected with either low titer (low), high titer (high), or ten-fold serial dilutions (serial) of phage as indicated.

during infection, we observed strong reduction in λ_{vir} titer but no effect on the plaque forming ability of a co-infecting M13 phage, even across a 10^7 -fold range of phage titers (Figure 3B, Supplementary Figure S7).

DISCUSSION

Although Cas12a is generally used to create staggered dsDNA breaks at specified sites, indiscriminate DNA and RNA shredding *in vitro* has been observed after target cleavage (15–17). This non-specific *trans*-cleavage has been repurposed for diagnostics, but it is not known if it occurs in cells or contributes to bacterial immunity. Here, we provide evidence that ssDNA *cis*- or *trans*-cleavage by Cas12a is insufficient to contribute to immunity against invasive ssDNA. LbCas12a did not detectably reduce ssDNA phage plaque formation or plasmid conjugation *in cis* or *in trans*, but it robustly targeted dsDNA elements encoding a PAM. We also saw no evidence of LbCas12a triggering cell dormancy or death, suggesting it does not sufficiently target host nucleic acids to cause toxicity. Cas12a targeting did not prevent the emergence of escapers or impact their ability to form plaques; however, we cannot exclude the possibility that Cas12a targeting slows the emergence of escapers.

The results shown here are consistent with previous reports showing high specificity and relatively infrequent off-target effects for Cas12a in cells (49–52). The reasons for undetectable *trans*-cleavage are unclear, but it may be due

to protection of ssDNA by DNA-binding proteins that exclude Cas12a or the rapid conversion of invasive ssDNA to dsDNA replicative forms (47,53–56). Consistent with this, ssDNA cleavage rates are not as high as initially reported and may be insignificant given the transient nature of naked ssDNA in the cell (24). Likewise, the protospacers used in this study are encoded on the template or coding strand of MGE regions that are expected to be transcribed, which may enable DNA or RNA polymerase to displace 'activated' Cas12a protein from its target.

Our inability to detect this activity in bacteria may also be due to the internal dynamics of Cas12a and crRNA assembly in cells. Cas12a has been shown to persist in a conformationally active state after target cleavage due to maintenance of the crRNA-DNA R-loop (19). High crRNA levels have been suggested to 'reset' LbCas12a after cleavage by releasing the R-loop, thus allowing Cas12a to revert to its conformationally 'closed' state. We were unable to test the impact of low crRNA levels on indiscriminate cleavage in our assays due to confounding impacts on dsDNA targeting, but this possibility remains. Alternatively, *trans*-cleavage may occur at levels too low to be detected in our assays or may be effectively repaired by the cell. An *in vivo* setting that more closely mimics the high levels of Cas12a and its target used *in vitro* may therefore allow for detectable collateral damage. Finally, it must be noted that the strains used here are not natural hosts for Type V-A CRISPR systems. Because native hosts for Cas12a are either genetically

intractable or lack tractable plasmids and phages, we opted to express inducible LbCas12a in *E. coli* and *P. aeruginosa* and test for ssDNA cleavage using plasmids and phages that infect these species. Although we did not observe *cis*- or *trans*-ssDNA cleavage across a range of conditions, it is possible that Cas12a ssDNAse activity exists only in its native hosts or against certain species of ssDNA.

Nonetheless, the rapid degradation of M13 ssDNA by Cas12a observed *in vitro* does not recapitulate *in vivo*, showing that CRISPR-Cas activities in cells cannot be understood through *in vitro* studies alone. Although indiscriminate cleavage activities *in vitro* have raised concerns about the use of Cas12a in gene editing, Cas12a has been generally regarded as an accurate enzyme in mammalian cells (57) and our results suggest the absence of rampant ssDNA cleavage during anti-phage/plasmid immunity. Cas12a therefore remains a powerful and versatile tool for the myriad of applications that already exist and are still to come.

DATA AVAILABILITY

All data and relevant information will be made available upon request.

SUPPLEMENTARY DATA

Supplementary Data are available at NAR Online.

ACKNOWLEDGEMENTS

We thank members of the Bondy-Denomy lab for thoughtful discussions, including Sukrit Silas for his experimental advice. We thank Jason M. Peters for the pTN7C185 vector and advice on strain engineering. We also thank Paul Bollyky, Joliene Sweere, Pat Secor and Alison Coluccio for their help with Pf4 phage. Author contributions: N.D.M. conceived of the project, engineered the bacterial strains and performed phage infection and *in vitro* experiments. R.P.-R. performed all conjugation experiments and made the figure schematics. N.D.M., R.P.-R. and J.B.-D. all contributed to experimental design and writing of the manuscript. J.B.-D. supervised the project.

FUNDING

N.D.M. was supported by the National Institutes of Health F32 [F32GM133127]; R.P.-R. was supported by the Lundbeck Foundation (Lundbeckfonden) postdoctoral grant [R347-2020-2346]; J.B.-D. was supported by the National Institutes of Health [DP5-OD021344, R01GM127489]. Funding for open access charge: National Institutes of Health [R01GM127489].

Conflicts of interest statement. J.B.-D. is a scientific advisory board member of SNIPR Biome and Excision Biotherapeutics and a scientific advisory board member and co-founder of Acrigen Biosciences. The Bondy-Denomy lab receives research support from Felix Biotechnology. J.B.-D. and N.D.M. have filed patents on technology related to Cas12a anti-CRISPR proteins.

REFERENCES

- Makarova, K.S., Wolf, Y.I., Iranzo, J., Shmakov, S.A., Alkhnbashi, O.S., Brouns, S.J.J., Charpentier, E., Cheng, D., Haft, D.H., Horvath, P. *et al.* (2020) Evolutionary classification of CRISPR-Cas systems: a burst of class 2 and derived variants. *Nat. Rev. Microbiol.*, **18**, 67–83.
- Strutt, S.C., Torrez, R.M., Kaya, E., Negrete, O.A. and Doudna, J.A. (2018) RNA-dependent RNA targeting by CRISPR-Cas9. *Elife*, **7**, e32724.
- Jiang, W., Samai, P. and Marraffini, L.A. (2016) Degradation of phage transcripts by CRISPR-associated RNases enables type III CRISPR-Cas immunity. *Cell*, **164**, 710–721.
- Abudayyeh, O.O., Gootenberg, J.S., Konermann, S., Joung, J., Slaymaker, I.M., Cox, D.B.T., Shmakov, S., Makarova, K.S., Semenova, E., Minakhin, L. *et al.* (2016) C2c2 is a single-component programmable RNA-guided RNA-targeting CRISPR effector. *Science*, **353**, aaf5573.
- Kazlauskienė, M., Tamulaitis, G., Kostiuik, G., Venclovas, Č. and Siksnys, V. (2016) Spatiotemporal control of type III-A CRISPR-Cas immunity: coupling DNA degradation with the target RNA recognition. *Mol. Cell*, **62**, 295–306.
- Lopatina, A., Tal, N. and Sorek, R. (2020) Abortive infection: bacterial suicide as an antiviral immune strategy. *Annu. Rev. Virol.*, **7**, 371–384.
- Rostøl, J.T., Xie, W., Kuryavyi, V., Maguin, P., Kao, K., Froom, R., Patel, D.J. and Marraffini, L.A. (2021) The cardI nuclease provides defence during type III CRISPR immunity. *Nature*, **590**, 624–629.
- McMahon, S.A., Zhu, W., Graham, S., Rambo, R., White, M.F. and Gloster, T.M. (2020) Structure and mechanism of a type III CRISPR defence DNA nuclease activated by cyclic oligoadenylate. *Nat. Commun.*, **11**, 500.
- Zhu, W., McQuarrie, S., Grüşchow, S., McMahon, S.A., Graham, S., Gloster, T.M. and White, M.F. (2021) The CRISPR ancillary effector can2 is a dual-specificity nuclease potentiating type III CRISPR defence. *Nucleic Acids Res.*, **49**, 2777–2789.
- Meeske, A.J., Nakandakari-Higa, S. and Marraffini, L.A. (2019) Cas13-induced cellular dormancy prevents the rise of CRISPR-resistant bacteriophage. *Nature*, **570**, 241–245.
- Zetsche, B., Gootenberg, J.S., Abudayyeh, O.O., Slaymaker, I.M., Makarova, K.S., Essletzbichler, P., Volz, S.E., Joung, J., van der Oost, J., Regev, A. *et al.* (2015) Cpf1 is a single RNA-guided endonuclease of a class 2 CRISPR-Cas system. *Cell*, **163**, 759–771.
- Paul, B. and Montoya, G. (2020) CRISPR-Cas12a: functional overview and applications. *Biomed. J.*, **43**, 8–17.
- Zetsche, B., Heidenreich, M., Mohanraju, P., Fedorova, I., Kneppers, J., DeGennaro, E.M., Winblad, N., Choudhury, S.R., Abudayyeh, O.O., Gootenberg, J.S. *et al.* (2017) Multiplex gene editing by CRISPR-Cpf1 using a single crRNA array. *Nat. Biotechnol.*, **35**, 31–34.
- Swarts, D.C. and Jinek, M. (2018) Cas9 versus cas12a/cpf1: Structure-function comparisons and implications for genome editing. *Wiley Interdiscip. Rev. RNA*, **9**, e1481.
- Chen, J.S., Ma, E., Harrington, L.B., Da Costa, M., Tian, X., Palefsky, J.M. and Doudna, J.A. (2018) CRISPR-Cas12a target binding unleashes indiscriminate single-stranded DNase activity. *Science*, **360**, 436–439.
- Li, S.-Y., Cheng, Q.-X., Liu, J.-K., Nie, X.-Q., Zhao, G.-P. and Wang, J. (2018) CRISPR-Cas12a has both *cis*- and *trans*-cleavage activities on single-stranded DNA. *Cell Res.*, **28**, 491–493.
- Fuchs, R.T., Curcuru, J., Mabuchi, M., Yourik, P. and Robb, G.B. (2019) Cas12a *trans*-cleavage can be modulated *in vitro* and is active on ssDNA, dsDNA, and RNA. bioRxiv doi: <https://doi.org/10.1101/600890>, 08 April 2019, preprint: not peer reviewed.
- Stella, S., Alcón, P. and Montoya, G. (2017) Structure of the cpf1 endonuclease R-loop complex after target DNA cleavage. *Nature*, **546**, 559–563.
- Stella, S., Mesa, P., Thomsen, J., Paul, B., Alcón, P., Jensen, S.B., Saligram, B., Moses, M.E., Hatzakis, N.S. and Montoya, G. (2018) Conformational activation promotes CRISPR-Cas12a catalysis and resetting of the endonuclease activity. *Cell*, **175**, 1856–1871.
- Swarts, D.C. and Jinek, M. (2019) Mechanistic insights into the *cis*- and *trans*-acting DNase activities of Cas12a. *Mol. Cell*, **73**, 589–600.
- Swarts, D.C., van der Oost, J. and Jinek, M. (2017) Structural basis for guide RNA processing and seed-dependent DNA targeting by CRISPR-Cas12a. *Mol. Cell*, **66**, 221–233.

22. Singh, D., Mallon, J., Poddar, A., Wang, Y., Tippana, R., Yang, O., Bailey, S. and Ha, T. (2018) Real-time observation of DNA target interrogation and product release by the RNA-guided endonuclease CRISPR *cpf1* (*Cas12a*). *Proc. Natl. Acad. Sci. U.S.A.*, **115**, 5444–5449.
23. Murugan, K., Seetharam, A.S., Severin, A.J. and Sashital, D.G. (2020) CRISPR-Cas12a has widespread off-target and dsDNA-nicking effects. *J. Biol. Chem.*, **295**, 5538–5553.
24. Ramachandran, A. and Santiago, J.G. (2021) CRISPR enzyme kinetics for molecular diagnostics. *Anal. Chem.*, **93**, 7456–7464.
25. Kaminski, M.M., Abudayyeh, O.O., Gootenberg, J.S., Zhang, F. and Collins, J.J. (2021) CRISPR-based diagnostics. *Nat. Biomed. Eng.*, **5**, 643–656.
26. Xu, X., Chemparathy, A., Zeng, L., Kempton, H.R., Shang, S., Nakamura, M. and Qi, L.S. (2021) Engineered miniature CRISPR-Cas system for mammalian genome regulation and editing. *Mol. Cell*, **81**, 4333–4345.
27. Yan, W.X., Hunnewell, P., Alfonse, L.E., Carte, J.M., Keston-Smith, E., Sothiselvam, S., Garrity, A.J., Chong, S., Makarova, K.S., Koonin, E.V. *et al.* (2019) Functionally diverse Type V CRISPR-Cas systems. *Science*, **363**, 88–91.
28. Carabias, A., Fuglsang, A., Temperini, P., Pape, T., Sofos, N., Stella, S., Erlendsson, S. and Montoya, G. (2021) Structure of the mini-RNA-guided endonuclease CRISPR-Cas12j3. *Nat. Commun.*, **12**, 4476.
29. Zhang, H., Li, Z., Xiao, R. and Chang, L. (2020) Mechanisms for target recognition and cleavage by the Cas12i RNA-guided endonuclease. *Nat. Struct. Mol. Biol.*, **27**, 1069–1076.
30. Wu, Z., Zhang, Y., Yu, H., Pan, D., Wang, Y., Wang, Y., Li, F., Liu, C., Nan, H., Chen, W. *et al.* (2021) Programmed genome editing by a miniature CRISPR-Cas12f nuclease. *Nat. Chem. Biol.*, **17**, 1132–1138.
31. Blattner, G., Cavazza, A., Thrasher, A.J. and Turchiano, G. (2020) Gene editing and genotoxicity: targeting the off-targets. *Front Genome Ed.*, **2**, 613252.
32. Swarts, D.C. (2019) Making the cut(s): how cas12a cleaves target and non-target DNA. *Biochem. Soc. Trans.*, **47**, 1499–1510.
33. Choi, K.-H. and Schweizer, H.P. (2006) mini-Tn7 insertion in bacteria with single attTn7 sites: example *Pseudomonas aeruginosa*. *Nat. Protoc.*, **1**, 153–161.
34. Choi, K.-H., Kumar, A. and Schweizer, H.P. (2006) A 10-min method for preparation of highly electrocompetent *Pseudomonas aeruginosa* cells: application for DNA fragment transfer between chromosomes and plasmid transformation. *J. Microbiol. Methods*, **64**, 391–397.
35. Hoang, T.T., Kutchma, A.J., Becher, A. and Schweizer, H.P. (2000) Integration-proficient plasmids for *Pseudomonas aeruginosa*: site-specific integration and use for engineering of reporter and expression strains. *Plasmid*, **43**, 59–72.
36. MacLean, R.C. and Buckling, A. (2009) The distribution of fitness effects of beneficial mutations in *Pseudomonas aeruginosa*. *PLoS Genet.*, **5**, e1000406.
37. Green, M.R. and Sambrook, J. (2017) Preparation of single-stranded bacteriophage M13 DNA by precipitation with polyethylene glycol. *Cold Spring Harb. Protoc.*, **2017**, db.prot093419.
38. Marino, N.D., Zhang, J.Y., Borges, A.L., Sousa, A.A., Leon, L.M., Rauch, B.J., Walton, R.T., Berry, J.D., Joung, J.K., Kleinstiver, B.P. *et al.* (2018) Discovery of widespread Type I and Type V CRISPR-Cas inhibitors. *Science*, **362**, 240–242.
39. Mo, C.Y., Mathai, J., Rostøl, J.T., Varble, A., Banh, D.V. and Marraffini, L.A. (2021) Type III-A CRISPR immunity promotes mutagenesis of *Staphylococci*. *Nature*, **592**, 611–615.
40. Hall, A.R., Iles, J.C. and Craig MacLean, R. (2011) The fitness cost of rifampicin resistance in *Pseudomonas aeruginosa* depends on demand for RNA polymerase. *Genetics*, **187**, 817–822.
41. Fonfara, I., Richter, H., Bratovič, M., Le Rhun, A. and Charpentier, E. (2016) The CRISPR-associated DNA-cleaving enzyme Cpf1 also processes precursor CRISPR RNA. *Nature*, **532**, 517–521.
42. Virolle, C., Goldlust, K., Djermoun, S., Bigot, S. and Lesterlin, C. (2020) Plasmid transfer by conjugation in Gram-negative bacteria: from the cellular to the community level. *Genes (Basel)*, **11**, 1239.
43. Secor, P.R., Burgener, E.B., Kinnersley, M., Jennings, L.K., Roman-Cruz, V., Popescu, M., Van Belleghem, J.D., Haddock, N., Copeland, C., Michaels, L.A. *et al.* (2020) Pf bacteriophage and their impact on *Pseudomonas* virulence, mammalian immunity, and chronic infections. *Front. Immunol.*, **11**, 244.
44. Tarafder, A.K., von Kùgelgen, A., Mellul, A.J., Schulze, U., Aarts, D.G.A.L. and Bharat, T.A.M. (2020) Phage liquid crystalline droplets form occlusive sheaths that encapsulate and protect infectious rod-shaped bacteria. *Proc. Natl. Acad. Sci. U.S.A.*, **117**, 4724–4731.
45. Hill, D.F., Short, N.J., Perham, R.N. and Petersen, G.B. (1991) DNA sequence of the filamentous bacteriophage Pfl. *J. Mol. Biol.*, **218**, 349–364.
46. Horiuchi, K. (1997) Initiation mechanisms in replication of filamentous phage DNA. *Genes Cells*, **2**, 425–432.
47. Mai-Prochnow, A., Hui, J.G.K., Kjelleberg, S., Rakonjac, J., McDougald, D. and Rice, S.A. (2015) Big things in small packages: the genetics of filamentous phage and effects on fitness of their host. *FEMS Microbiol. Rev.*, **39**, 465–487.
48. Semenova, E., Kuznedelov, K., Datsenko, K.A., Boudry, P.M., Savitskaya, E.E., Medvedeva, S., Beloglazova, N., Logacheva, M., Yakunin, A.F. and Severinov, K. (2015) The cas6e ribonuclease is not required for interference and adaptation by the *E. coli* type I-E CRISPR-Cas system. *Nucleic Acids Res.*, **43**, 6049–6061.
49. Kleinstiver, B.P., Tsai, S.Q., Prew, M.S., Nguyen, N.T., Welch, M.M., Lopez, J.M., McCaw, Z.R., Aryee, M.J. and Joung, J.K. (2016) Genome-wide specificities of CRISPR-Cas Cpf1 nucleases in human cells. *Nat. Biotechnol.*, **34**, 869–874.
50. Kim, D., Kim, J., Hur, J.K., Been, K.W., Yoon, S.-H. and Kim, J.-S. (2016) Genome-wide analysis reveals specificities of Cpf1 endonucleases in human cells. *Nat. Biotechnol.*, **34**, 863–868.
51. Tóth, E., Weinhardt, N., Bencsura, P., Huszár, K., Kulcsár, P.I., Tálás, A., Fodor, E. and Welker, E. (2016) Cpf1 nucleases demonstrate robust activity to induce DNA modification by exploiting homology directed repair pathways in mammalian cells. *Biol. Direct*, **11**, 46.
52. Tu, M., Lin, L., Cheng, Y., He, X., Sun, H., Xie, H., Fu, J., Liu, C., Li, J., Chen, D. *et al.* (2017) A ‘new lease of life’: FnCpf1 possesses DNA cleavage activity for genome editing in human cells. *Nucleic Acids Res.*, **45**, 11295–11304.
53. Wawrzyniak, P., Plucienniczak, G. and Bartosik, D. (2017) The different faces of rolling-circle replication and its multifunctional initiator proteins. *Front. Microbiol.*, **8**, 2353.
54. Attaiech, L., Olivier, A., Mortier-Barrière, I., Soulet, A.-L., Granadel, C., Martin, B., Polard, P. and Claverys, J.-P. (2011) Role of the single-stranded DNA-binding protein SsbB in pneumococcal transformation: maintenance of a reservoir for genetic plasticity. *PLoS Genet.*, **7**, e1002156.
55. Marceau, A.H. (2012) Functions of single-strand DNA-binding proteins in DNA replication, recombination, and repair. In: *Single-Stranded DNA Binding Proteins*. Humana Press, Totowa, NJ, pp. 1–21.
56. Meyer, R.R. and Laine, P.S. (1990) The single-stranded DNA-binding protein of *Escherichia coli*. *Microbiol. Rev.*, **54**, 342–380.
57. Wei, Y., Zhou, Y., Liu, Y., Ying, W., Lv, R., Zhao, Q., Zhou, H., Zuo, E., Sun, Y., Yang, H. *et al.* (2021) Indiscriminate ssDNA cleavage activity of CRISPR-Cas12a induces no detectable off-target effects in mouse embryos. *Protein Cell*, **12**, 741–745.